Computer Assisted Methods in Engineering and Science, **22**: 347–363, 2015.

Mathematical modelling of heat transport in a section of human forearm

Oliwia Nowakowska, Zbigniew Buliński
Institute of Thermal Technology
Silesian University of Technology
Konarskiego 22, 44-100 Gliwice, Poland
e-mail: zbigniew.bulinski@polsl.pl

The paper presents numerical analysis of heat transfer in the human forearm and influence of its internal structure on the temperature distribution inside. For this purpose three geometrical models of a human forearm were developed: model containing continuous muscle tissue only, model in which muscle tissue and bones were considered and model which contained muscle tissue bones and main blood vessels. In those models heat transfer in the muscle tissues and bones were described by Pennes bioheat equation, while for blood flowing through main vessels (artery and vein) full set of governing equations were solved. Moreover, simplified one-dimensional description of skin was developed in order to reduce model complexity. Results obtained with all models were confronted against each other to reveal influence of the main blood vessels on the temperature distribution in a forearm.

Keywords: bioheat transfer, Pennes' equation, human forearm, temperature distribution, simplified skin model.

Nomenclature

ρ	–	density [kg/m^3],
c_p	–	specific heat at constant pressure [J/(kgK)],
c_B	–	specific heat of blood at constant pressure [J/(kgK)],
λ	–	thermal conductivity [W/(m K)],
$\boldsymbol{x}$	–	position vector [m],
t	–	time [s],
Q_{perf}	–	volumetric heat source due to blood perfusion [W/m^3],
Q_{met}	–	volumetric heat source due to cellular metabolism [W/m^3],
T	–	static temperature [K],
G	–	perfusion ratio [1/s],
α	–	heat transfer coefficient [W/m^{2}K],
∇	–	nabla differential operator,
$\boldsymbol{v}$	–	velocity vector [m/s],
$\boldsymbol{g}$	–	gravitational acceleration [m/s^2],
p	–	pressure [Pa],
μ	–	dynamic viscosity coefficient [kg/(ms)],
Φ	–	energy dissipation rate [kg/(m^{2}s^2)],
A	–	surface area [m^2],
L	–	length [m].

Subscripts

t – tissue,
B – blood,
s – skin surface,
0 – ambient,
st – subcutaneous tissue.

1. Introduction

Heat exchange in a living tissue is a very complicated process. The most commonly used mathematical model describing this phenomenon is the Pennes' equation. The main disadvantage of this equation is that it treats all blood vessels in a similar way regardless of their size and shape. In the Pennes' model, the heat transfer due to the blood flowing through the tissue is averaged over the tissue volume and the true blood vessel geometry is neglected. This crucial assumption of the Pennes' model is valid for small blood vessels, but in the case of large blood vessels it may result in considerable error.

Human beings are warm-blooded animals; therefore, their body must reach a balance between production of appropriate amount of heat within the body and releasing an excess heat to the surrounding environment. The balance is achieved by the advanced mechanisms of temperature control: change of metabolism and contraction and expansion of blood vessels in order to decrease or increase the amount of heat transferred due to perfusion. These processes must keep the core body temperature at level of 36–37°C [2]. This is in contrast to the poikilothermic organisms, whose internal temperature varies considerably with external temperature. In extremely cold conditions, these organisms can even lapse into lethargy to decrease heat losses [1]. Heat transfer between a living individual and the surroundings occurs mainly through the skin. This process is a complex phenomenon, which consists of a few coupled heat transfer mechanisms, namely: conduction, convection, radiation and a perspiration which consists of separation and evaporation of sweat [10, 15].

Nowadays, measurements of human body temperature are becoming more and more popular in medicine. They enable diagnosis of various diseases. For example, the studies of thermal processes have found their application in the following medical treatments:

- cryosurgery, which consists of destruction of abnormal or diseased tissue by the application of extreme cold,
- radiofrequency thermal ablation – a process of destruction of infected cells by application of high temperature,
- thermal resection – a process cutting the ill or infected cells using high temperature.

All these procedures destroy sick tissues by using thermal load; however, to carry out precisely such an operation the knowledge of mechanisms of heat transport in a living tissue is required.

Generally, temperature field in human body depends on the following factors: environmental conditions, temperature of surrounding tissues, muscle metabolism and blood circulation. As it has been already mentioned, heat exchange with the surrounding occurs primarily through the skin. Figure 1 shows schematically a cross-section of the subsequent layers of human body. Generally, the following main layers of the body can be distinguished: skin, fat, muscle, and bone. The skin includes two layers: epidermis and dermis [31]. At the external surface of epidermis heat is released to the surrounding by: convection, radiation and perspiration (see Fig. 1).

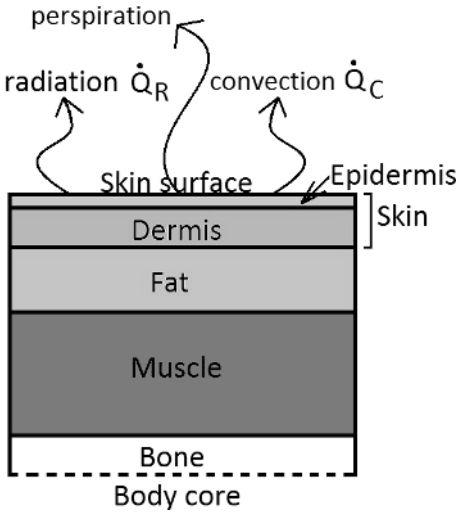

Fig. 1. The cross-section through the subsequent layers of human body [31].

Inside the living tissue, heat transfer occurs by conduction (less important mechanism) and by advection due to microscopic and macroscopic blood flow through a network of blood vessels, this mechanism is commonly called perfusion. The primary function of a blood circulatory system in a body is the transport of oxygen and nutrients. The second important function of the circulatory system is heat transport and active temperature control in deep parts of the body. The heat generated in the body by metabolism, especially in its deep organs, is transported by the blood perfusion to the skin surface and then it is further released to the environment by convection, radiation and perspiration.

Blood begins its circulation in the heart, which it exits through the aorta, the largest artery. Blood is supplied to the organs and muscles by smaller branches of arteries, called arterioles. After a delivery of nutrients through the blood system of veins, the blood goes to the vena cava, the largest vein in the circulatory system. From the main vein, the blood goes straight to the heart. Arterioles and veins form a mesh of blood vessels called capillaries. It is worth to mention that the diameter of the veins can be up to 100% larger than the diameter of their artery counterparts [11, 13, 18]. In the large blood vessels the blood behaves as a Newtonian fluid [20].

In Fig. 2, a schematic distribution of blood temperature as a function of blood vessel size is shown. The blood leaving the heart has a deep body temperature T_{a0}, which may considerably

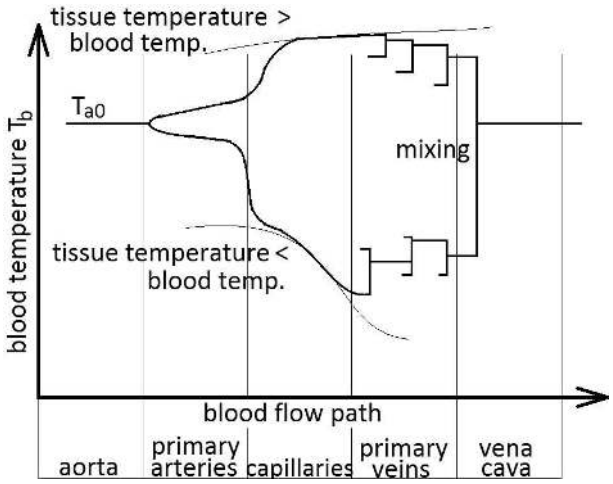

Fig. 2. The schematic of temperature distribution in different blood vessels [11].

differ from a local tissue temperature, then an intense heat exchange between blood and tissue takes place. If the temperature of the surrounding tissue is higher than the blood temperature then the blood temperature increases. Otherwise, the initial blood temperature decreases. As the blood flows into the vessels with smaller diameter the heat exchange between blood and tissue is enhanced due to an increase of effective heat exchange area. This results in slow equalization of both temperatures and the system slowly converging to the thermal equilibrium condition. This process can be depicted as a mixing process. By contrast, while the diameter of the vessel increases on its way back to the heart, the difference between the blood and tissue temperatures increases [11, 18].

2. Literature review

The mathematical modelling of heat flow in a body has been the subject of the intense research since the mid-twentieth century, and since then it has become more popular mainly due to an increasing interest in the possibilities of application of heat in medical treatment of many illnesses. One of the first formal mathematical descriptions of heat transfer processes in living tissues was given by Pennes [19]. Pennes assumed ideal thermal mixing of blood and surrounding tissue, which resulted in ideal equalization of blood and tissue temperatures. Pennes used his mathematical model to compute the radial temperature distribution in a forearm and he confronted obtained numerical results with the results of measurements. In contrary to Pennes' approach, the mathematical model proposed by Wulff assumed that the heat flow exchanged between blood and tissue is proportional to the temperature difference between these two mediums [30]. Similar model was proposed by Klinger [12]. One of the most advanced mathematical models of heat transfer in human body was proposed by Chen and Holmes [7]. They applied the idea of local thermal non-equilibrium and wrote a separate energy equation for blood and tissue. However, their model neglected the effect of counter-current blood flow in veins and arteries. This effect was addressed in the works of Weinbaum et al. [27, 28]. A comprehensive review of all the mentioned models can be found in many works, for example, Telega et al., Valvano, and Zolfaghari et al. [23, 26, 31], just to mention a few.

Although the Pennes' bioheat equation has a few shortcomings, it is commonly used to model the heat flow in human body. One of the first practical applications of Pennes' bioheat equation considered heat transfer in skin subjected to fire [24]. This problem was further developed to a multilayer one by Majchrzak et al. [16]. Trobec and Depoli developed a mathematical model of heat flow in the adult forearm [25]. Their model was based on the Pennes' equation, however they used a very accurate geometrical information on the interior structure of the forearm available through the Visual Human Project [4]. They compared their numerical results with the experimental data published by Pennes. The mathematical model of heat transport in the infant body was developed by Łaszczyk et al. [5]. Ciesielski et al. analysed the heat flow in 2D cross-section of the human forearm with use of control volume method [8]. Duda et al. modelled the heat transfer in the 3D section of the human forearm [9]. They used a very reliable geometry of the internal structure of the forearm including subsequent tissue layers, bones and main blood vessels; however, they neglected the blood flow in vessels and treated it just as a boundary condition.

This paper presents transport mathematical modelling of heat and blood flow in a section of adult forearm. Developed mathematical model includes the elements typical in macroscopic as well as microscopic heat flow in human body. The main goal of this work is to verify computationally the influence of the presence of blood flow in large blood vessels, e.g., the main artery and vein in the arm. Similar approach to modelling of heat transfer in a living tissue was presented by Stańczyk et al. [21, 22]. The authors, in those publications, applied the discreet vessel segmentation methodology developed by Kotte et al. [14] to include 1D blood flow through vessels. In this paper, mathematical model of a forearm section of an individual adult was developed. The scope of this work included developing the forearm geometry, preparing numerical mesh and building mathematical model, and carrying out calculations. The ANSYS FLUENT computational fluid dynamics (CFD) software was used to build the numerical model and to carry out the computations.

Three different models with different level of forearm internal complexity were built. This allowed us to examine the influence of the forearm internal structure (in particular the presence of bones, main blood vessels and skin) on the temperature distribution.

2.1. Pennes' equation of bioheat transfer

As it was already mentioned, Pennes' equation is one of the first mathematical models describing the heat flow in living tissues. It is also one of the most commonly applied models in describing the heat flow and the temperature distribution in living tissues. The key assumptions of this model can be summarized as follows:

- Capillary bed equilibration. The only independent variable of the Pennes' bioheat equation is a tissue temperature. The primary heat exchange between tissue and blood takes place in the capillary bed (arterioles and venules). Blood flowing through the capillaries reaches thermal equilibrium with surrounding tissue. The heat exchange between the blood flowing through larger vessels and the tissue is neglected.

- Blood perfusion. It is assumed that blood flow is isotropic, hence the blood flow direction is neglected and the effects such as countercurrent blood flow in arteries and veins cannot be included in the model.

- Vascular architecture. Geometrical shape and dimensions of the blood vessels are ignored.

- Blood temperature. It is assumed that blood enters the capillary bed with deep body temperature (core temperature) and leaves at tissue temperature.

The crucial, in this list, is the assumption that the primary heat exchange takes place in the capillary bed, and the heat exchange in all other blood vessels can be neglected. The remaining points actually can be inferred from this point. To verify these assumptions, Pennes studied experimentally temperature inside the human forearm in a few cross-sections downstream from the elbow [19]. Investigations were carried out at ambient air temperatures of 25–27°C. Measurements of temperature were made along transverse axis of the forearm using specially prepared thermocouples placed inside a needle. Pennes' studies have shown that arterial blood has a higher temperature of the tissue. Blood flow heats not only the tissues between the skin and the axis of the arm, but also the surface of the skin. The results showed that the temperature difference between the skin and the hand interior was equal to 3 to 4°C. This difference is caused by metabolic heat generation and perfusion of blood. Based on the research, Pennes suggested an equation of heat transfer in the human body, which includes the heat release due to metabolism and the heat transport due to blood perfusion [19]:

$$\rho \cdot c \cdot \frac{\partial T}{\partial t} = \nabla \cdot [\lambda(T) \nabla T] + Q_{\text{perf}} + Q_{\text{met}}, \tag{1}$$

where T is tissue temperature, the coefficient c refers to a specific heat of tissue, ρ is tissue density, λ stands for the heat conduction coefficient of tissue. Finally, Q_{perf} and Q_{met} denote the volumetric heat source due to perfusion and metabolism. With the assumptions given above, the volumetric heat source due to perfusion can be expressed as

$$Q_{\text{perf}} = \rho_B \cdot c_B \cdot G_B \cdot [T_B - T], \tag{2}$$

where ρ_B is the blood density, c_B denotes a specific heat of blood at constant pressure, G_B is the volumetric blood flow rate per unit volume (perfusion rate), and T_B refers to the blood temperature entering capillary bed, which is equal to the core body temperature.

The Pennes' equation quite realistically models heat transfer processes between tissue and small vessels (capillary bed). Moreover, an important advantage of the Pennes' equation is that the perfusion term is linear with respect to temperature, which allows for the analytical solution of the equation in certain geometric cases. Considerable disadvantages of this equation are the simplifying assumptions regarding capillary bed equilibration, blood perfusion, vascular architecture and blood temperature as listed above. Due to these shortcomings many researchers disputed the Pennes' model and proposed alternative approaches. Today, we have much better computational tools and more accurate data. But, the analysis of heat flow inside a living tissue and its modelling still remain an open topic, even after all this time since the first publication of the Pennes' model [26]. In this work, advanced CFD tools are used to verify the influence of large blood vessels on the tissue temperature.

3. Mathematical model

The considered numerical model included a fragment of the adult forearm from the wrist to the elbow with length of 23 cm. In order to accomplish the main goal, namely to verify the influence of the internal structure of the forearm, three geometrical models were developed. The first of them considered homogenous muscle tissue and neglected the arm internal structure. In the second model two bones were included, namely: ulna and radius. Additionally, the third model included the forearm main blood vessels: the cephalic vein and radial artery. In the following chapter details of the developed numerical and mathematical models will be presented.

3.1. Geometrical models

The analysed geometrical models were based on the dimensions of the forearm of an adult. Firstly, the forearm was measured at several places, and then the measurements were transferred as consecutive cross-sections of the forearm to the DS CATIA V5R20 CAD software. Next, the defined sections of the forearm were used to create the lateral surface. After its closure, a solid model of the forearm was created. The first model, created in this way, which included muscle tissue only, is shown in Fig. 3.

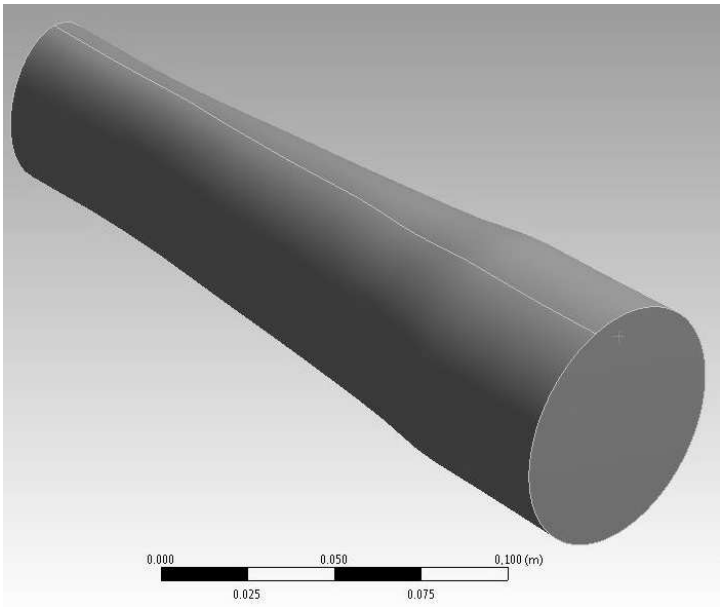

Fig. 3. Geometry of the first considered model.

The second model was extended by inclusion of the two bones – the radius and the ulna with diameters of 12 mm and 15 mm, respectively. Its final geometry is shown in Fig. 4.

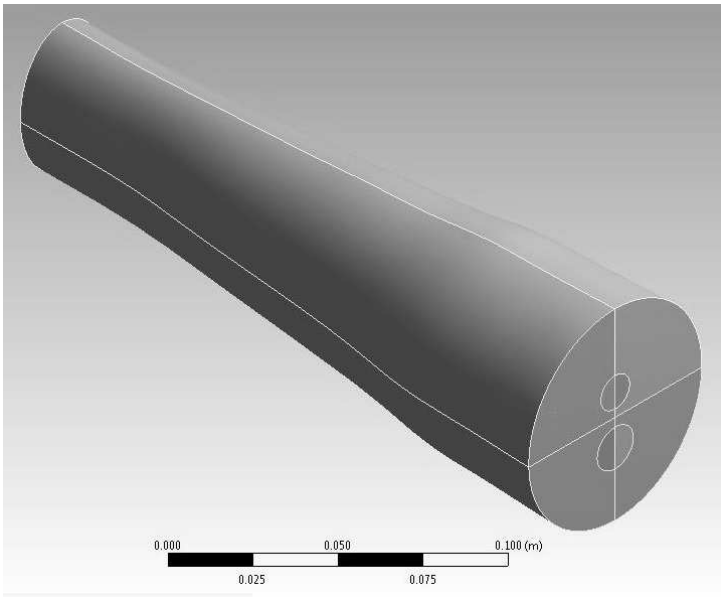

Fig. 4. Geometry of the second considered model including radius and ulna.

The third model is shown in Fig. 5, and in comparison to the second model, it additionally includes two larger blood vessels: the cephalic vein and the radial artery. Their diameters were assumed as: artery – 3.5 mm [17] and vein – 1.8 mm [3]. In the numerical computations, it was assumed that the blood flowing in the vessels is not flashing, which means that the expansion of blood vessels was not considered in this work.

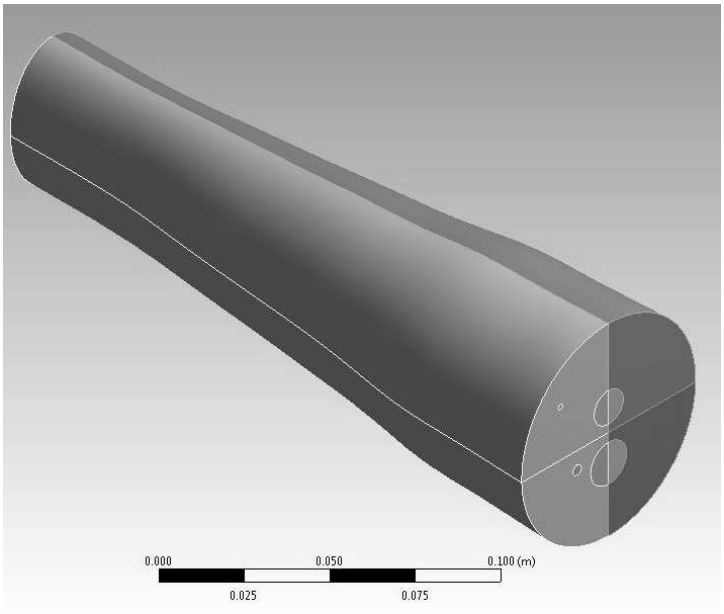

Fig. 5. Geometry of the third considered model including two blood vessels.

Figures 3–5 show the models which were imported into ANSYS Workbench Design Modeler. These models were imported into ANSYS Workbench environment and specially processed to be

able to create numerical grid, namely all the short edges and small faces were removed. The numerical grid was built using ANSYS Mesher software. Due to the relatively regular shape of all models, it was possible to create the grid containing prisms and hexahedral elements. Boundary layer was located at the surface of the skin what resulted in better reproduction of the temperature gradient. Obtained numerical grids were characterized by very high quality. An example of numerical grid for the most complicated model is presented in Fig. 6.

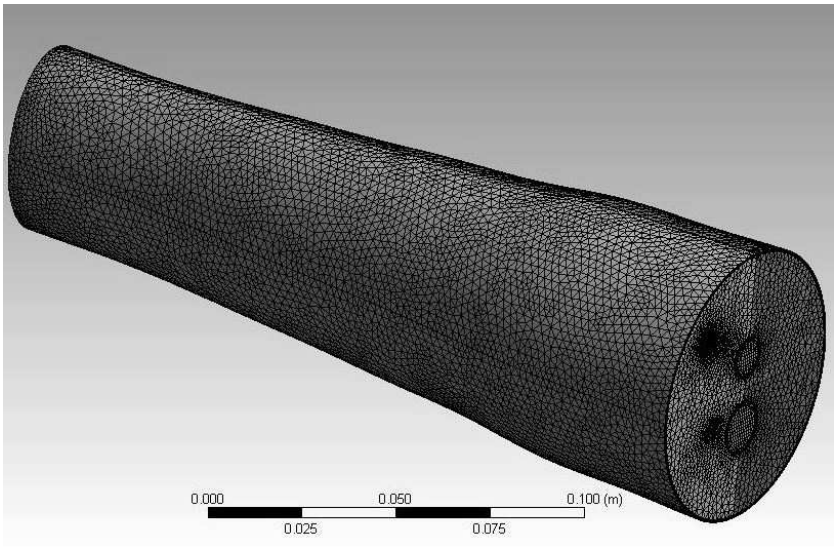

Fig. 6. Numerical grid in model with muscle tissue, bones and blood vessels.

3.2. Boundary conditions

In order to obtain a particular solution of the boundary value problem (BVP) it is necessary to define boundary conditions. In the case of heat transfer problem, these conditions include information about the temperature field and its derivatives (in the form of heat flow). The analyses were carried out for steady state conditions, therefore there was no need to specify the initial temperature distribution. Boundary conditions were given for the outer skin surface and for the two surfaces, where the forearm has been virtually cut off. It was assumed that the skin surface is flown past by the air with a temperature equal to 26°C. Moreover, forced convection was assumed at this surface with the heat transfer coefficient at level of 16 W/m^{2}K. Hence, mathematically this can be written as

$$-\lambda_t \frac{\partial T}{\partial n}|_{b_{\mathrm{III}}} = \alpha \cdot (T_S - T_{\mathrm{inf}}), \tag{3}$$

where $\dfrac{\partial}{\partial n}|_{b_{\mathrm{III}}}$ is a derivative in the normal direction to the skin outer surface b_{III} on which this boundary condition was assigned [6], T_S is the temperature of the skin outer surface while T_{inf} stands for the air temperature.

The boundary condition of the second type was applied at the surfaces where the considered forearm section was cut off. It means that the heat flux in a normal direction to those surfaces is known and equal to zero:

$$-\lambda_t \cdot \frac{\partial T}{\partial n}|_{b_{\mathrm{II}}} = 0, \tag{4}$$

where b_{II} stands for the boundary at which second type boundary condition was assigned.

3.3. Equations describing heat flow in living tissues

Three mathematical models developed in this work differ in the accuracy of interior geometry reproduction. The first model considers only muscle tissue, in the second model bones are included. The third model considers muscle tissue, bones and blood flow in main vessels. Calculations for all three models were carried out with and without skin model. Heat transfers in all tissues, namely muscle, bones and skin, were described by Pennes' equations (1) with appropriate values of perfusion and metabolic heat. As it was already mentioned Pennes' equation is not appropriate to describe the heat transfer in large blood vessels. Therefore, in the third case, in which large blood vessels were modelled explicitly, a full set of flow equations consisting of continuity, momentum conservation and energy conservation equations, was solved.

3.4. The equations describing the blood flow in blood vessels

For the most complex geometrical model, it was assumed that the blood which flows into the artery has the inlet temperature of 310 K, which is close to the deep body temperature. It was also assumed that this temperature does not change with time. Moreover, it was assumed that the temperature of blood which flows into the vein section has the temperature equal to the temperature of blood outflowing from the artery section. Determining the temperature of blood to flowing into the vein was carried out using the user defined functions – UDFs. Moreover, in the developed model it was assumed that the blood behaves as an incompressible Newtonian fluid [20].

- ***The continuity equation***

The general principle of mass conservation tells us that the mass can not disappear or be formed in any point of the field. This principle for an incompressible fluid, wherein the density of fluid is constant will be fulfilled if the velocity divergence is zero. Hence, differential form of continuity equation can be written as follows [29]:

$$\nabla \cdot \mathbf{v}_B = 0, \tag{5}$$

where $\mathbf{v}_B$ is the blood velocity vector.

- ***The momentum conservation equation***

The general principle of conservation of momentum writes that the fluid contained in the moving control volume causes a momentum change equal to the resultant of the external forces acting on the fluid. For an incompressible Newtonian fluid this equation has the following form [29]:

$$\rho_B \frac{D\mathbf{v}_B}{Dt} = \rho_B \mathbf{g} - \nabla p_B + \mu_B \nabla^2 \mathbf{v}_B, \tag{6}$$

where ρ_B is the blood density, $\mathbf{g}$ stands for gravitational acceleration, p_B denotes pressure and μ_B is the blood viscosity. In the carried out analyses, it was assumed that viscosity has constant value.

- ***The energy conservation equation***

The general principle of energy conservation states that energy enclosed in moving control volume is equal to the energy exchanged by heat transfer and work with the surrounding. For an incompressible Newtonian fluid this results in the following differential equation [29]:

$$\rho_B \cdot c_B \frac{dT_B}{dt} = \lambda_B \nabla^2 T_B + \Phi, \tag{7}$$

where λ_B is the heat conductivity of blood and Φ refers to energy dissipation rate due to viscous friction in the fluid.

3.5. 1D skin model

In Fig. 1, a simplified internal structure of the human body is presented, in which the following subsequent layers can be distinguished: skin (dermis and epidermis), subcutaneous tissue (fat), muscle and bone. This approximately reconstructs the internal forearm structure. However, a technical problem arises in a numerical modelling of such a multilayered structure, namely some layers are very thin compared to others. For example, epidermis thickness is below 0.1 mm, dermis around 2 mm and fat between 1–10 mm. Direct geometrical modelling of such thin layers would result in large numerical grid and it would deteriorate considerably the quality of this grid, especially for the cells close to the boundaries of those layers. For this reason, the dermis and subcutaneous tissue layers were not modelled directly but the solution of 1D bioheat equation was used to describe the heat flow through these two layers. Practically, this results in prescribing local heat flux at the external skin surface obtained by the solution of 1D bioheat equation in those two layers. This was carried out by the use of the UDFs. The problem is presented schematically in Fig. 7. The true boundary for the numerical model is the surface between muscle tissue and subcutaneous tissue, heat flux at this boundary is prescribed by using the developed UDF. As a result of numerical calculations carried out by FLUENT, the temperature T_t, obtained at the surface, is an input for the UDF computing the heat flux.

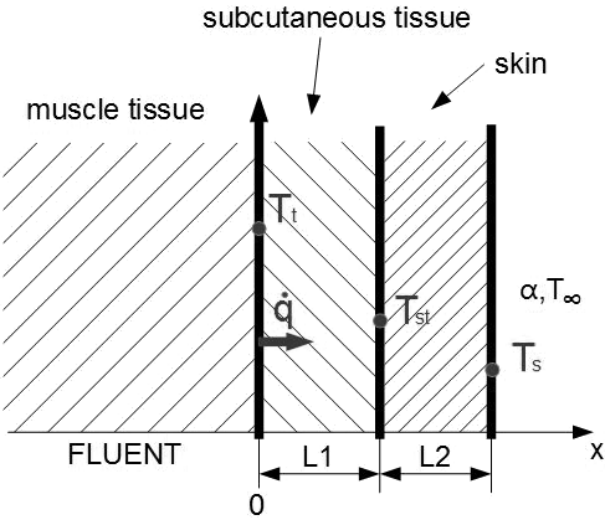

Fig. 7. Schematic of the cross-section model.

The second available information, that enables to compute the heat flux at the muscle tissue, is the heat flow condition at the outer skin surface. In this work, it is assumed that the heat transfer coefficient α and the undisturbed air temperature T_{inf} are known at this surface. Having this information one can write four equations for the heat fluxes between consecutive layers:

1. The heat flux at the outer skin surface is calculated using a Newton equation

$$q(x = l_1 + l_2) = \alpha(T_s - T_{\text{inf}}). \tag{8}$$

2. The heat flux at the outer skin surface (obtained from the analytical solution of 1D Pennes' equation in the skin layer [6]) is

$$q(x = l_1 + l_2) = -\lambda_s m_s \cdot \frac{(T_s - A_s) \cdot \cosh(m_s l_2) - (T_{st} - A_s)}{\sinh(m_s l_2)}. \tag{9}$$

3. The heat flux at the surface between skin and subcutaneous tissue (obtained from the analytical solution of 1D Pennes' equation in the skin layer [6]) is

$$q(x = l_1) = -\lambda_s m_s \cdot \frac{(T_s - A_s) - (T_{st} - A_s) \cdot \cosh(m_s l_2)}{\sinh(m_s l_2)}. \tag{10}$$

4. The heat flux at the surface between skin and subcutaneous tissue (obtained from the analytical solution of 1D Pennes' equation in the subcutaneous layer [6]) is

$$q(x = l_1) = -\lambda_{st} m_{st} \cdot \frac{(T_{st} - A_{st}) \cdot \cosh(m_{st} l_1) - (T_t - A_{st})}{\sinh(m_{st} l_1)}, \tag{11}$$

where $q(x = l_1 + l_2)$ and $q(x = l_1)$ are the heat fluxes at skin outer surface and the surface between subcutaneous tissue and skin respectively. T_s refers to the outer skin temperature, T_{st} denotes the temperature at the surface between subcutaneous tissue and skin, λ_s and λ_{st} are the heat conductivities of skin and subcutaneous tissue and A_s and A_{st} are reduced temperatures of skin and subcutaneous tissue, described by formula:

$$A_i = T_a + \frac{Q_{\mathrm{met},i}}{G_{B,i}\rho_B c_B}, \tag{12}$$

where T_a denotes blood temperature in the aorta which is assumed to be equal to deep body temperature and m_{st} and ms are the parameters described by:

$$m_i = \sqrt{\frac{G_{B,i}\rho_B c_B}{\lambda_i}}, \tag{13}$$

where $i = st, s$.

Assuming that muscle tissue temperature, heat transfer coefficient and ambient temperature are known, there are four unknowns in Eqs. (8)–(11), namely two heat fluxes: $q(x = l_1 + l_2)$ and $q(x = l_1)$, temperature T_{st} between subcutaneous tissue and skin, and the outer skin temperature T_s. Rearranging this set of four Eqs. (8)–(11) one can obtain the expression for heat flux at the surface between muscle tissue and subcutaneous tissue $q(x = 0)$:

$$q(x = 0) = -\lambda_{st} m_{st} \cdot \frac{(T_{st} - A_{st}) - (T_t - A_{st}) \cdot \cosh(m l_1)}{\sinh(m l_1)}. \tag{14}$$

Equation (14) is called at the beginning of each iteration and for given muscle tissue temperature read from the solver that calculates the heat flux which is prescribed at the muscle tissue surface.

3.6. Parameters of simulation

In the carried out computations it was assumed that the physical properties are constant. The values of physical properties of all tissues that are present in the developed model are given in Table 1. Values of the parameters of the Pennes' bioheat equation used in the mathematical model were assumed after the work of Trobec and Depoli [25]. It was assumed that these parameters have constant values corresponding to temperature of 310 K (see Table 2). Although in reality a bone is comprised of outer cortical tissue and interior trabecular tissue, in this work the values corresponding to cancellous bone were prescribed for the whole bone region.

Moreover, for the computation purpose, it was assumed that inlet artery temperature is equal to 310 K, while the heat transfer coefficient on the external skin surface was assumed to be equal to 16 W/m^{2}K and the ambient temperature was 299.15 K.

Table 1. Characteristic properties of individual structures.

Factor	Heat conduction coefficient λ [W/mK]	Specific heat capacity c [J/kgK]	Density ρ [kg/m^3]
Skin	0.51	3431	1200
Subcutaneous tissue	0.55	2241	812
Muscle tissue	1.03	4668	1179
Cancellous bone	0.5	2260	900
Blood	0.67	3890	1057

Table 2. Properties of blood perfusion and metabolism.

Factor	Blood flow T_s [ml/100 ml·min]	Blood perfusion [m^3/m^3·s]	Metabolic heat Q_{met} [W/m^3]
Skin	2.823	0.000188	385.838
Subcutaneous tissue	2.823	0.000188	261.084
Muscle tissue	2.823	0.000376	758.173
Cancellous bone	2.823	0.000282	289.379

4. Results

In the following subsection, the results of the numerical computations of heat and blood flow in the section of the adult forearm are presented. The results obtained for all analysed cases are compared in term of temperature distribution at the external skin surface and temperature distribution at the longitudinal and traverse forearm cross-sections. Traverse cross-sections were located along the forearm in regular intervals of 4.6 cm.

4.1. Comparison of different forearm models

In Figs. 8 and 9, a variation of temperature field inside the forearm and at its surface can be observed. It can also be noticed that the simplest model including muscle tissue only gives results very similar to the second model with muscles and bones. In the case of those two models the lowest temperature occurs in the vicinity of the wrist while the highest temperature appears in the axis of the forearm. Significantly different is the temperature distribution obtained with the most complex model which includes muscle tissue, bones and blood flow in the principal vessels. In contrary to both simpler models, in this model the highest temperature occurs in the blood vessels. Moreover, the influence of the presence of large blood vessels on the local temperature field inside the muscle tissue is clearly visible. Although, similarly to two simpler models, the lowest temperature is at the skin surface near the wrist, and the influence of blood flow in the vessels is seen at the external skin surface.

4.2. Skin model influence

The purpose of simplification of the skin in the forearm numerical model was to save computational resources and time. Thin layers of skin and subcutaneous tissue would enforce a very fine grid in

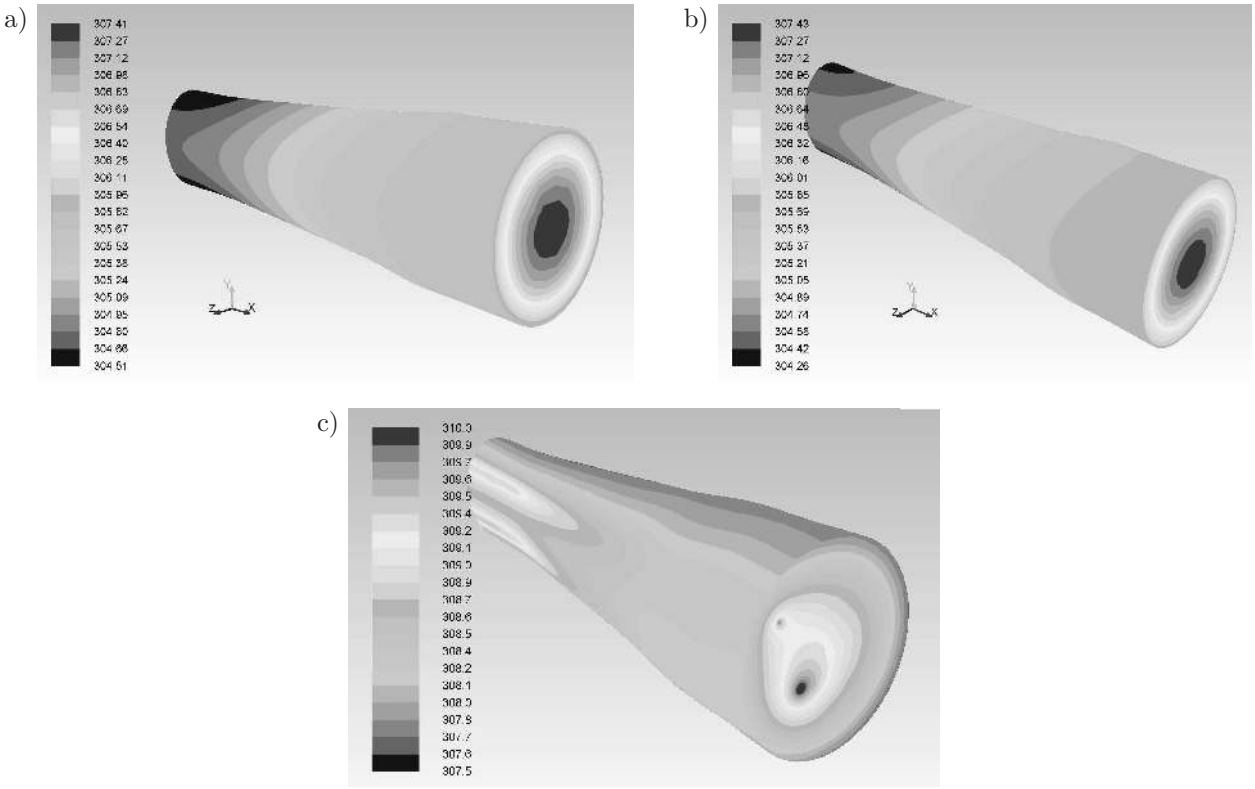

Fig. 8. The results for the model of the forearm without skin: a) model including muscle tissue only, b) model with bones, c) model with blood vessels.

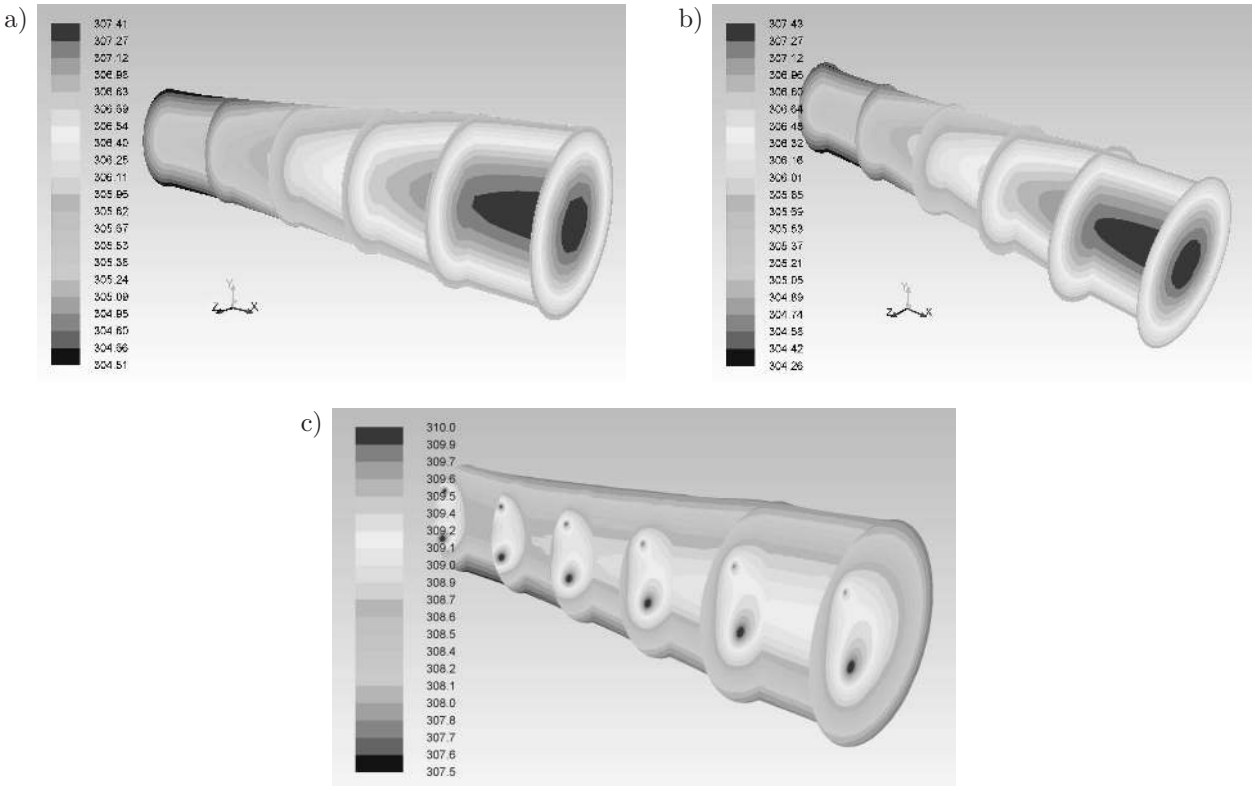

Fig. 9. The results for the model of the forearm without skin (sections): a) model including muscle tissue only, b) model with bones, c) model with blood vessels.

those layers, thus making the model significantly bigger. In Fig. 10, distributions of temperature fields at the outer surfaces of the model are compared. It can be seen that, qualitatively, inclusion of the skin does not influence the temperature distribution at the outer skin surface. In all three geometrical models, temperature fields reveal the same characteristic features such as the position of maximum and minimum temperature or the influence of internal forearm structure. There are, however, some differences in the temperature range between the corresponding models with and without the skin model. These differences are presented in Table 3, where the maximum

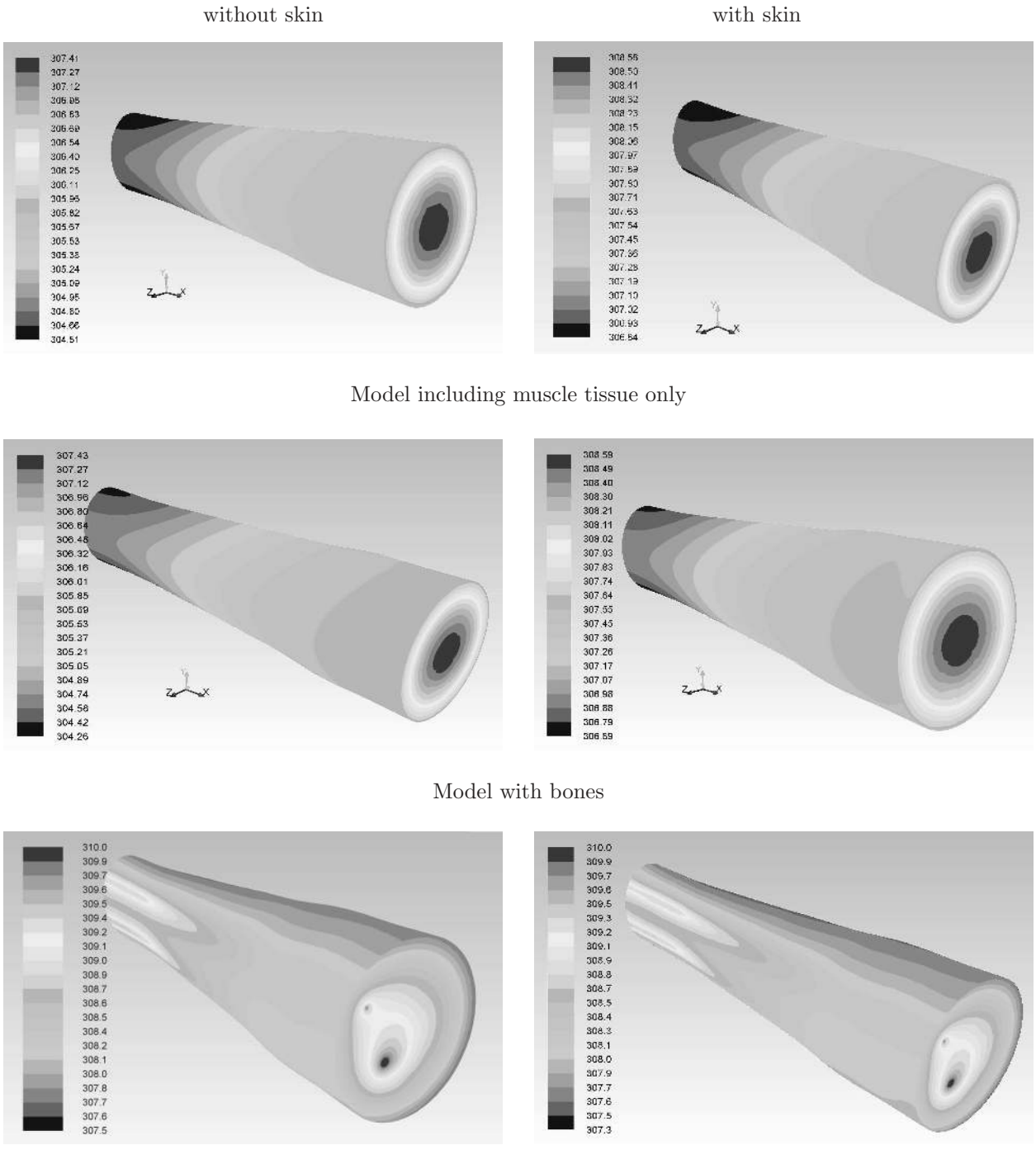

Fig. 10. Comparison of temperature fields for models with and without the skin.

Table 3. Comparison of minimum and maximum temperature values obtained in models with and without the skin.

	Temperatures T [C]			
	with skin		without skin	
	max	min	max	min
Model including muscle tissue only	35.43	33.69	34.26	31.36
Model with bones	35.44	33.54	34.28	31.11
Model with bones and blood vessels	36.85	34.35	36.85	34.15

and minimum temperatures obtained in the models with skin and without skin are compared with each other. In the case of the model which includes the skin, temperatures are slightly higher than in the model without the skin. This is noticeable for the maximum and the minimum temperature values and is caused by the insulating properties of the skin. Moreover, the difference between the maximum and minimum temperatures is more pronounced in the simplest model, in which only a muscle tissue is considered. The skin inclusion to the most complex model does not influence the maximum temperature because it is the temperature of blood at the inlet of the artery.

5. Summary

This paper presents the analysis of heat transport and blood flow in a section of the adult forearm. The Pennes' bioheat equation was applied to describe the heat flow in the continuous tissues (muscle, bone, etc.) and the blood flow in the vessels was modelled directly by solving blood flow equations. Analyses were performed for three models with different level of representation of internal forearm structure. The basic model included muscle tissue only, and in the second model two main forearm bones were added. The third and the most complex model included blood vessels: artery and vein. Moreover, in this model the blood flow in the vessels was modelled directly by solving flow equations. It was assumed that the heat exchange between a human and the environment occurred only by convection. In the analysis, the heat radiation and the evaporation of sweat from the skin surface were neglected.

It was shown that in comparison to the simplest model, the presence of bones almost does not influence the temperature distribution. The temperature field at the forearm cross-section in the first and second model has the same concentric character with the highest value in the forearm axis. On the contrary, in the case of the model with blood vessels, the temperature field looks entirely different because the highest temperature appears in the entire length of the vein and artery. This is caused by the strong convection between blood flowing in the vessels and surrounding tissue. Such an effect was preliminary confirmed by infrared measurements of skin temperature. Thermograms in Fig. 11 reveal that places where the blood vessel runs close to the skin surface have a distinctively higher temperature. In the case of all models, the carried out computations have shown a temperature drop along the forearm, however this effect needs closer examination.

The addition of the skin in all studied models does not influence significantly the temperature distribution. The skin acts as an insulator causing that the resulting temperatures are higher than in the models without the skin.

Further work on this topic will include the development of more detailed geometric model based on cross-sections of the entire human body, which is available in the Visible Human Project [4]. In addition, the analysis will be extended to other mechanisms of heat exchange with the environment.

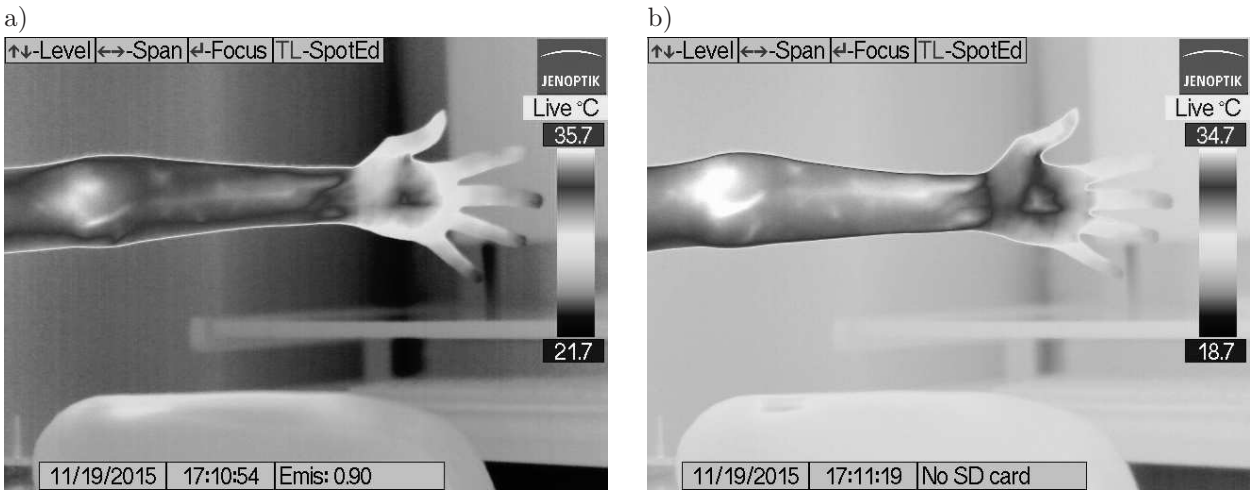

Fig. 11. Thermal images of the forearm.

References

[1] *Anatomy and physiology – cool-blooded animals (poikilotherms)*. The Columbia Electronic Encyclopedia, 6th ed., Columbia University Press available on the internet: http://www.infoplease.com/encyclopedia/science/body-temperature-cold-blooded-animals-poikilotherms.html [accessed on 07.02.2016].

[2] *Medical dictionary – warm-blooded*. The Free Dictionary by Farlex. Available on the internet: http://medical-dictionary.thefreedictionary.com/Warm+blooded [accessed on 07.02.2016].

[3] *Handbook of basic clinical procedures* [in Polish: *Podręcznik podstawowych zabiegów klinicznych*]. Available on the internet: http://edu.pam.szczecin.pl/~marcinm/INIEKCJE.html [accessed on 15.12.2015].

[4] *The Visible Human Project*, U.S. National Library of Medicine, 2003. Available on the internet: https://www.nlm.nih.gov/research/visible/visible_human.html [accessed on 18.12.2015].

[5] J. Łaszczyk, A. Maczko, W. Walas, A.J. Nowak. Inverse thermal analysis of the neonatal brain cooling process. *International Journal of Numerical Methods for Heat & Fluid Flow*, **24**(4): 946–968, 2014.

[6] T.L. Bergman, A.S. Lavine, F.P. Incorpera, D.P. DeWitt. *Fundamentals of heat and mass transfer*. John Wiley & Sons, 6th ed., 2008.

[7] M.M. Chen, K.R. Holmes. Microvascular contributions in tissue heat transfer. *Annals of the New York Academy of Sciences*, **335**: 137–150, 1980.

[8] M. Ciesielski, B. Mochnacki. Application of the control volume method using the Voronoi polygons for numerical modeling of bio-heat transfer processes. *Journal of Theoretical and Applied Mechanics*, **52**(4): 927–935, 2014.

[9] M. Duda, B. Mochnacki. 3D model of thermal interactions between human forearm and environment. *Journal of Applied Mathematics and Computational Mechanics*, **14**(3): 17–23, 2015.

[10] K.C. Gokul, D.B. Gurung, P.R. Adhikary, Effect of blood perfusion and metabolism in temperature distribution in human eye. *Advances in Applied Mathematical Biosciences*, **4**(1): 13–23, 2013.

[11] L.M. Jiji. *Heat Conduction*, pp. 302–304, Springer, Berlin, 2009.

[12] H.G. Klinger, Heat transfer in perfused biological tissue. I. General theory. *Bulletin of Mathematical Biology*, **36**(4): 403–415, 1974.

[13] A. Kucaba-Piętal. *Blood as complex fluid, flow of suspensions*. [In:] Blood Flow Modelling and Diagnostics. Advanced Course and Workshop – BF 2005, Warsaw, June 20–23, 2005, T.A. Kowalewski [Ed.], pp. 9–30, Institute of Fundamental Technological Research, Polish Academy of Sciences, Warsaw, 2005.

[14] A. Kotte, G. van Leeuwen, J. de Bree, J. van der Koijk, H. Crezee, J. Lagendijk. A description of discrete vessel segments in thermal modelling of tissues. *Physics in Medicine and Biology*, **41**(5): 865, 1996, http://stacks.iop.org/0031-9155/41/i=5/a=004.

[15] M. Krause, *Thermoregulation of the human body and thermal load* [in Polish: *Termoregulacja organizmu człowieka i obciążenie termiczne*]. Centralny Instytut Ochrony Pracy, Wrocław, 2004.

[16] E. Majchrzak, B. Mochnacki, M. Jasiński, Numerical modelling of bioheat transfer in multi-layer skin tissue domain subjected to a flash fire. *Computational Fluid and Solid Mechanics*, **1–2**: 1766–1777, 2003.

[17] M. Misterski. *Evaluation of selected methods of radial artery extraction in direct myocardial revascularization* [in Polish: *Ocena wybranych sposobów pobierania tętnicy promieniowej w operacjach bezpośredniej rewaskularyzacji mięśnia sercowego*]. Poznań, 2008, available on the internet: http://www.wbc.poznan.pl/dlibra/plain-content?id=92412 [accessed on 15.12.2015].

[18] A. Narasimhan. The role of porous medium modeling in biothermofluids. *Journal of the Indian Institute of Science*, **91**: 343–366, 2011.
[19] H.H. Pennes, Analysis of tissue and arterial blood temperatures in the resting human forearm. *Journal of Applied Physiology*, **1**(2): 93–122, 1948.
[20] D. Quemada, *Blood rheology and its implication in flow of blood*. Laboratoire de Biorheologie et Universite Paris VII, pp. 3–9, 1983.
[21] M. Stańczyk. Vascular model of heat transfer in perfused tissue. [In:] Blood Flow Modelling and Diagnostics. Advanced Course and Workshop – BF 2005, Warsaw, June 20–23, 2005, T.A. Kowalewski [Ed.], pp. 451–487, Institute of Fundamental Technological Research, Polish Academy of Sciences, Warsaw, 2005.
[22] M. Stańczyk, G.M.J. Van Leeuwen, A.A. Van Steenhoven, Discrete vessel heat transfer in perfused tissue – model comparison. *Physics in Medicine and Biology*, **52**(9): 2379, 2007.
[23] M. Stańczyk, J.J. Telega. Modelling of heat transfer in biomechanics – a review. Part I. Soft tissues. *Acta of Bioengineering and Biomechanics*, **4**(1): 31–61, 2002.
[24] D.A. Torvi, J.D. Dale. A finite element model of skin subjected to a flash fire. *ASME Journal of Biomechanical Engineering*, **116**(3): 250–255, 1994.
[25] R. Trobec, M. Depolli, Simulated temperature distribution of the proximal forearm. *Computers in Biology and Medicine*, **41**(10): 971–979, 2011.
[26] J.W. Valvano, *Bioheat Transfer*, The University od Texas at Austin, pp. 19–23, Austin, USA.
[27] S. Weinbaum, L.M. Jiji. A new simplified bioheat equation for the effect of blood flow on local average tissue temperature. *ASME Journal of Biomechanical Engineering*, **107**: 131–139, 1985.
[28] S. Weinbaum, L.M. Jiji, D.E. Lemons, Theory and experiment for the effect of vascular microstructure on surface tissue heat transfer. Part I. Anatomical foundation and model conceptualization. *ASME Journal of Biomechanical Engineering*, **106**: 321–330, 1984.
[29] F.M. White, *Fluid Mechanics*, 6th ed., pp. 338–342, McGraw-Hill, 2006.
[30] W. Wulff, The energy conservation equation for living tissues. *IEEE Transactions-Biomedical Engineering*, **21**(6): 494–495, 1974.
[31] A. Zolfaghari, M. Maerefat, *Bioheat Transfer*, pp. 155–156, InTech, http://cdn.intechweb.org/pdfs/19889.pdf, 2011.